



Mechanics Based Design of Structures and Machines

An International Journal

ISSN: (Print) (Online) Journal homepage: <https://www.tandfonline.com/loi/lmbd20>

Semi-automatic retractable handrail utilizing opening/closing movement of sliding door supporting elderly people to walk independently: Strength analysis of sliding door and experimental verification

Kinjiro Saitou, Nao-Aki Noda, Yoshikazu Sano, Yasushi Takase, Zefeng Wang, Shuqiong Li, Hiroyuki Tanaka & Yoshitaka Kubo

To cite this article: Kinjiro Saitou, Nao-Aki Noda, Yoshikazu Sano, Yasushi Takase, Zefeng Wang, Shuqiong Li, Hiroyuki Tanaka & Yoshitaka Kubo (2023): Semi-automatic retractable handrail utilizing opening/closing movement of sliding door supporting elderly people to walk independently: Strength analysis of sliding door and experimental verification, *Mechanics Based Design of Structures and Machines*, DOI: [10.1080/15397734.2023.2168692](https://doi.org/10.1080/15397734.2023.2168692)

To link to this article: <https://doi.org/10.1080/15397734.2023.2168692>



Published online: 23 Jan 2023.



Submit your article to this journal [↗](#)



View related articles [↗](#)



View Crossmark data [↗](#)



Semi-automatic retractable handrail utilizing opening/closing movement of sliding door supporting elderly people to walk independently: Strength analysis of sliding door and experimental verification

Kinjirou Saitou^a, Nao-Aki Noda^b, Yoshikazu Sano^b, Yasushi Takase^b, Zefeng Wang^{b,c}, Shuqiong Li^b, Hiroyuki Tanaka^b, and Yoshitaka Kubo^d

^aYahata Rolling Mechanical Engineering Department, Engineering Division, Mechanical Engineering Unit, Nippon Steel Texeng Co., Ltd, Fukuoka, Japan; ^bDepartment of Mechanical Engineering, Kyushu Institute of Technology, Fukuoka, Japan; ^cShandong Jiaotong University, Changqing District, Jinan City, China; ^dArchitecture Engineering Department, Development Division, Kei Products Co., Ltd, Fukuoka, Japan

ABSTRACT

The sliding door with the retractable handrail examined in this study can be installed in hospitals and nursing facilities for helping the elderly and disabled to walk independently. This provides the prospect of restoring their declining walking abilities. In this study, wood is not used as building construction, which is common usage, but as mechanical structure. Though the strength evaluation is required, there is no clear standard for the fatigue strength of wood. Hence, this study shows the method of calculating the yield strength and fatigue limit of wood by investigating the methods of calculating allowable stresses in ASTM and AIJ, which are intended to be used for building construction. Using the result, the maximum tensile stress σ_{\max}^T and the maximum compressive strength σ_{\max}^C on the installation part of the handrail bar mounting plate where the risk is the highest are obtained by the finite element method (FEM). It is shown to be safe for the static strength and fatigue strength above.

ARTICLE HISTORY

Received 6 October 2021
Accepted 3 January 2023

KEYWORDS

Sliding door; handrail; plywood; ratio of fatigue limit endurance ratio; people with disabilities

1. Introduction

Sliding doors have a lot of advantages compared to hinged doors widely used throughout the world. People can have a greater sense of spaciousness because no additional area is required for opening the door, and the door is tucked into the wall, leaving the doorway fully unobstructed. Additionally, the sliding doors are suitable for the elderly because only a light sliding motion of pulling or pushing is required to open or close the door. As shown in Fig. 1, houses, hospitals, and welfare facilities for the elderly or handicapped who need nursing care, or those in poor health, are equipped with handrails over the entire length of the corridors so that they can grab and walk without the assistance of care givers.

Preventing a decline in walking ability helps maintain and restore ability when an unhealthy person is able to walk independently (Gault and Willems 2013; Porter, Vandervoort, and Lexell 1995; World Health Organization 2007). However, if there is a sliding door in the middle of the corridor, it is not possible to install a general handrail. In order to support independent living, it

CONTACT Nao-Aki Noda  noda.naoaki844@mail.kyutech.jp 
Communicated by Francisco Javier González Varela.

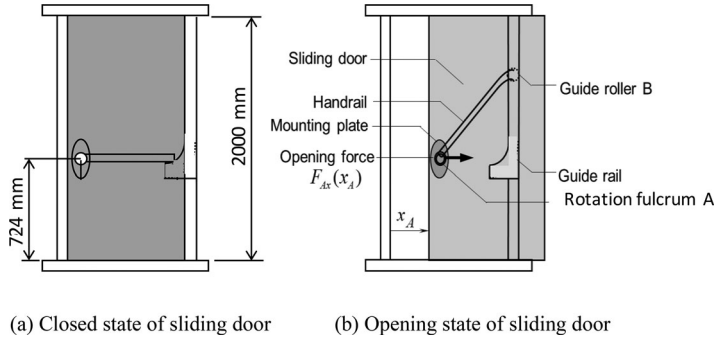


Figure 1. Illustration of sliding door with retractable handrail.

is necessary to install handrails continuously without interruption, eliminate the risk of falling while walking, and increase the motivation to walk (Arfken et al. 1994; Chu et al. 1999; Cumming et al. 2000; Gunter et al. 2000; Howland et al. 1998; Kim et al. 2001; Lachman et al. 1998). In terms of structural design purposes of constructions, such doors, sliding components, secondary systems, etc. are required to satisfy specific performance demands that are strictly related to primary buildings they belong. Thus, for example under seismic events, the investigated sliding doors should possibly avoid or minimize potential risk for building occupants (Bedon, Amadio, and Noè 2019).

Figure 1 illustrates a sliding door with a retractable handrail (Kubo 2010, 2017). In the previous study, a formula was derived to obtain the opening force of the sliding door with the handrail. Simulations using the equation showed that the maximum opening force is consistent with the experiment by a difference of 13%, and the difference can be reduced if necessary (Saitou et al. 2021). The target of this study is to confirm that the sliding door can withstand 2×10^5 times of repeated use and is sufficiently safe for strength. This is important for the users without sufficient physical abilities. The target number of repeated uses is twice as many times as the allowable number of uses of sliding doors specified in the requirement (1×10^5 times, JIS A 4702:2000).

The plywood in the area where the mounting plate is attached is checked to see if it withstands the designed target for repeated load, 2×10^5 times. This number of repeated operations is twice as many times as the allowable number of uses of sliding doors specified in the requirement (1×10^5 times, JIS A 4702:2000) and more than twice as many times as that of aluminum window sashes specified in the requirement (3×10^4 times, JIS A 4706:2000).

2. Measurement and simulation of sliding door opening force using prototype

2.1. Structure of sliding door device

As shown in Fig. 1(b), the sliding door device with the retractable handrail consists of a sliding door, mounting plate, handrail, guide roller B, and guide rail. When the sliding door is closed as shown in Fig. 1(a), the retractable handrail functions as a handrail. The opening motion of the sliding door drives the guide roller B at the end of the handrail upward along the rolling surface inside of the guide rail stand while the rotation fulcrum A of the mounting plate works as an axis for the handrail. Conversely, the closing motion drives the handrail downward along the surface. Fig. 1(a) also shows the typical dimensions of the sliding door.

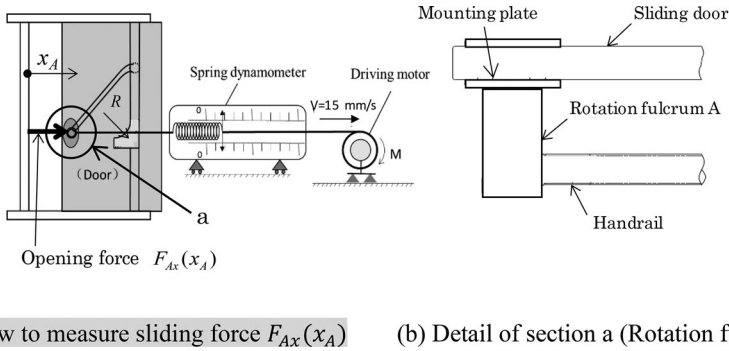


Figure 2. Measuring sliding force $F_{Ax}(x_A)$.

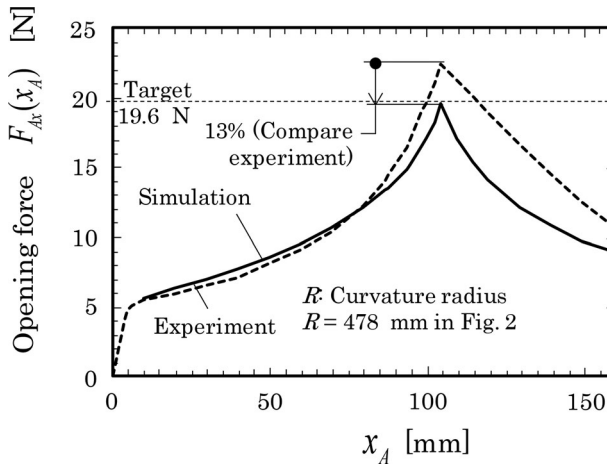


Figure 3. Sliding force $F_{Ax}(x_A)$ obtained theoretically and experimentally with door shown in Fig. 1.

2.2. Measurement and simulation of sliding door opening force

As shown in Fig. 2, the sliding door opening force $F_{Ax}(x_A)$ of the prototype was measured using a spring scale. For measurements, the spring scale was fixed on a bench which was installed on a horizontal plate flush with the mounting plate where the friction is negligible. A string connected to the end of the spring was pulled at a rate of 15 mm/second while the other end of the spring was fixed on the mounting plate side. Figure 3 shows the measurement results for the geometry of the prototype handrail and guide rail, shown in Fig. 4. The simulation analysis here is based on a theoretical value obtained from the equilibrium formula for the force indicated in Appendix A. Comparing the experimental result with the result derived from the equilibrium formula, the experimental and theoretical maximum values are 22.4 N and 19.5 N respectively when $R=478$ mm. It was confirmed that they match within a 13% difference. These results are in line with the previous studies (Saitou et al. 2018, 2021).

3. Fatigue limit estimation for wood materials and plywood

ASTM D245-06 (2019) and ASTM D2555-17a (2017) describe a strength evaluation method for American wood. In Japan, the Architectural Institute of Japan (AIJ) provides the standards for wood materials in "Standard for structural design of timber structures" (AIJ 2006) with ASTM as

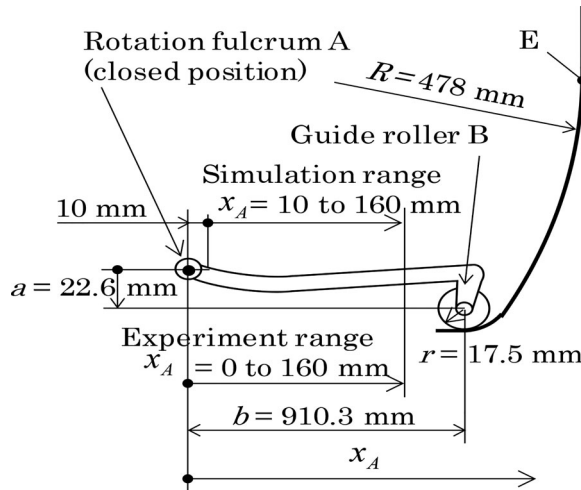


Figure 4. Geometry of prototype handrail and guide rail.

a guide. However, neither ASTM nor AIJ includes the strength at fatigue limit σ_w or endurance ratio σ_w/σ_B required for the strength study on mechanical design. First, this paper describes the overview of each adjustment coefficient in ASTM and AIJ, which is used for strength evaluation of structural plywood used in this study. The reasons why the coefficients are selected are also included. Then, it also describes that the product of coefficients α_f , which will be explained later, can be considered as endurance ratio σ_w/σ_B . Endurance ratios σ_w/σ_B derived from the strength evaluation methods in two standards, ASTM and AIJ, are compared and studied.

3.1. Comparison between ASTM and AIJ

Though ASTM D245-06 (2019) specifies the strength evaluation method for lumber, no strength evaluation equation is found for plywood. On the other hand, the method of AIJ can be used for the strength evaluation both in lumber and plywood. Since AIJ includes the coefficient of degradation influence, which considers degradation due to UV and moisture for the lumber strength specific to plywood, AIJ allows plywood to be evaluated in strength. This paper evaluates the strength of plywood not only based on AIJ but on ASTM by applying the same coefficient of degradation influence as AIJ. The two standards are then compared. The strength of the plywood used for the sliding door in this study will be confirmed to satisfy the evaluation standards both in ASTM and AIJ. Product of coefficients α_f , the product of various adjustment coefficients obtained here, is used for the strength evaluation. Table 1 shows the calculation methods for coefficients to reduce the static strength of plywood with ASTM D245 and AIJ. Note that the values in Table 1 are for plywood made of softwood. The wood material evaluated here is the first-grade structural plywood material 15 mm thick made of softwood (sugi) specified in Japanese agricultural standard (JAS). The specification details for the sliding door plywood can be found in Section 4.1.

As shown in Table 1, the ASTM strength evaluation method for lumber uses adjustment factor α_a , degradation factor α_{a1} , strength ratio α_b , seasoning adjustment α_c , and special factor α_e . As described above, in this study, the product of these is additionally multiplied by environmental coefficient α_d in AIJ. This was determined as the strength evaluation method for plywood. On the other hand, the AIJ calculation method uses adjustment factor α_a , degradation factor α_{a1} , safety factor α_{a2} , and environmental coefficient α_d . Since AIJ does not use strength ratio α_b , seasoning adjustment α_c , or special factor α_e , these coefficients are 1.0. These strength evaluation methods

Table 1. Method for calculating σ_w/σ_B from coefficients α_a to α_f defined in ASTM and AIJ when load duration is 250 years^e.

Coefficients	Bending		Tension parallel to grain		Compression parallel to grain	
	ASTM	AIJ	ASTM	AIJ	ASTM	AIJ
(a) Adjustment factor α_a in ASTM, $\alpha_a = (a1) \times (a2)$ in AIJ	1/2.2	1/3	1/2.2	1/3	1/2.0	1/3
(a1) Degradation factor α_{a1} in ASTM and AIJ	0.57 ^a	0.5	0.57 ^a	0.5	0.57 ^a	0.5
(a2) Safety factor α_{a2} in AIJ (equivalent to $\sigma_y/\sigma_B =$ ratio of yield strength to static strength ($\alpha_{a2} = \sigma_y/\sigma_B$))	(1/1.25) ^b	2/3	(1/1.25) ^b	2/3	(1/1.14) ^b	2/3
(b) Strength ratio α_b prescribed in ASTM	1.0	(1.0) ^b	1.0 × 0.55	(1.0) ^b	1.0	(1.0) ^b
(c) Seasoning adjustment α_c prescribed in ASTM	1.0	(1.0)	1.0	(1.0)	1.0	(1.0)
(d) Environmental coefficient α_d prescribed in AIJ	(3/4) ^c	3/4	(6/7) ^c	6/7	(6/7) ^c	6/7
(e) Special factors α_e prescribed in ASTM	1.0	(1.0) ^b	(1.0) ^b	(1.0) ^b	(1.0) ^b	(1.0) ^b
(f) Product of coefficients $\alpha_f = \alpha_a \times \alpha_b \times \alpha_c \times \alpha_d \times \alpha_e$ (Equivalent to $\sigma_w/\sigma_B =$ ratio of alternating fatigue limit to static strength ($\sigma_w/\sigma_B = \alpha_f$))	0.34	0.25^d	0.21^d	0.29	0.43	0.29^d

Values are for plywood made of soft wood.

^aThe values of α_a in ASTM are calculated setting the load duration at 250 years according to AIJ.

^bValues not prescribed in ASTM or AIJ are in parentheses.

^cSince α_d value for plywood is not prescribed in ASTM, the value in AIJ is indicated.

^dThe values recommended by the authors are shown in **bold** type.

^eAlthough the values in this table are for the first-grade structural plywood material 15 mm thick made of softwood (sugi) specified in JAS, this method can be applied to plywood made of hardwood.

based on ASTM and AIJ are detailed below. The strength evaluation methods shown here can also be applied to plywood made of hardwood. Additionally, it can be applied to lumber by excluding environmental coefficient α_d , which is only used for plywood.

3.2. Adjustment factor α_a , degradation factor

α_{a1} , and safety factor α_{a2} (ratio of yield strength to static strength ($\alpha_{a2} = \sigma_y/\sigma_B$))

This section describes adjustment factor α_a , degradation factor α_{a1} , and safety factor α_{a2} for ASTM and AIJ in Table 1. AIJ provides adjustment factor α_a as the product of degradation factor α_{a1} and safety factor α_{a2} ($\alpha_a = \alpha_{a1} \times \alpha_{a2}$). In AIJ, safety factor α_{a2} is used to reduce the allowable strength of a material to the elastic limit. On the other hand, ASTM only provides α_a and α_{a1} while α_{a2} is not included. The degradation factor α_{a1} is a coefficient determined by the duration of the load applied to the wood, and is derived from Fig. 5 (Nakamura, Yamasaki, and Murata 2015). Figure 5 shows degradation factor α_{a1} specified in ASTM D245, which is known as the Madison curve (Wood 1951). The curve is based on the bending test results of small clear wood specimens by Forest Products Laboratory in Madison, Wisconsin. The small clear wood specimen is a specimen in green condition without any defects, and ASTM D2555-17a (2017) specifies its strength value.

In this curve, the strength with various load durations is shown referring to the static strength with 10 minutes as 100%. The horizontal axis is a logarithmic axis of load duration. The solid line shows the ASTM values. Degradation factor α_{a1} at 50 years, the maximum load duration in ASTM, is used for the design. The broken line shows degradation factor α_{a1} from AIJ, which is shown in the standards (AIJ 2003, 2006). The straight line connecting point S at 10 minutes of load duration and point M at 3 months prescribed in ASTM shows degradation factor α_{a1} for AIJ. Degradation factor α_{a1} at 250 years, the maximum load duration, is used for the design. For comparison, the maximum load duration of degradation factor α_{a1} for ASTM should be changed to 250 years, the same duration as AIJ. The following describes the detailed values. First, adjustment factors α_a in ASTM are considered. The factors α_a to be applied to the strength of softwood small clear wood specimens at the load duration of 50 years are as follows: α_a for bending and

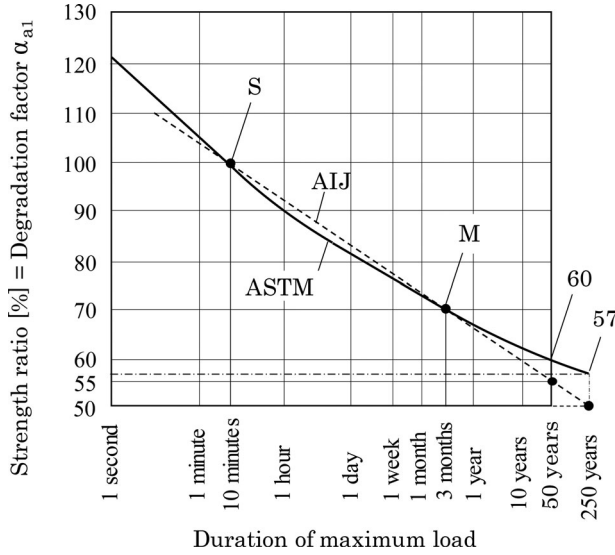


Figure 5. Relationship of degradation factor α_{a1} to duration of load in ASTM and AIJ.

tension = $1/2.1$, α_a for compression = $1/1.9$. Then, the load duration of 50 years is changed to the same load duration as AIJ, 250 years. In other words, adjustment factors α_a at 250 years are obtained using degradation factors α_{a1} at 50 years and 250 years: α_a for bending and tension = $(0.57/0.60) \times (1/2.1) = 1/2.2$, α_a for compression = $(0.57/0.60) \times (1/1.9) = 1/2.0$. Using these values, the ASTM safety factor α_{a2} for bending and tension can be calculated as follows. Since adjustment factor $\alpha_a = 1/2.2$ and degradation factor $\alpha_{a1} = 0.57$, safety factor $\alpha_{a2} = 1/(2.2 \times 0.57) = 1/1.25$ (Nakamura, Yamasaki, and Murata 2015). For compression, the calculation using $\alpha_a = 2.0$ and $\alpha_{a1} = 0.57$ gives the result $\alpha_{a2} = 1/1.14$. On the other hand, in AIJ, degradation factor α_{a1} at the load duration of 250 years is 0.5. Safety factor α_{a2} is $2/3$. AIJ specifies the value of degradation factor α_{a1} for bending, tension, and compression as the same value as safety factor α_{a2} . Their adjustment factor $\alpha_a = 0.5 \times 2/3 = 1/3$ is obtained.

3.3. Strength ratio α_b

Strength ratio α_b is a reduction factor specified in ASTM D245, which takes defects such as knots and cracks on full-sized lumber into account. Small clear wood specimens do not have these defects. To determine the allowable stresses of full-sized lumber, considering these defects, the strength obtained with the small clear wood specimen should be lowered by multiplying it by a coefficient corresponding to reasonable defects. The ratio that lowers the strength based on the kind of the defect and its size is called strength ratio. Defects include knots, slopes of grain, and cracks. For strength ratio α_b , the defect that increases the rate of lowering the strength the most should be selected from the defects.

In the standard of the JAS first-grade structural plywood (C-C grade) materials, which is used in this study, the knot size is specified at 50 mm or less. As shown in Table B2 where the strength is compared between L-axis and T'-axis, since plywood mitigates anisotropy of raw wood and is insusceptible to slopes of grain, strength ratio α_b is set to 1.0. AIJ specifies static strength σ_B where the shape and the number of defects are limited for each grade of wood. Therefore, in AIJ, strength ratio α_b for knots is included in static strength σ_B . Since strength ratios α_b for bending and compression in ASTM and those for bending, tension, and compression in AIJ are considered to be included in static strength σ_B for the JAS first-grade structural plywood material, they

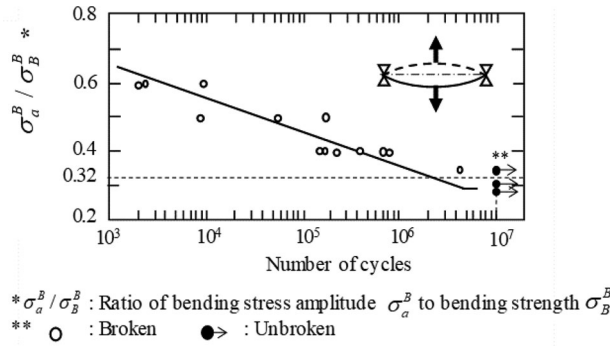


Figure 6. S-N curve of three-point bending fatigue for Japanese sugi.

are set to 1.0. Note that since strength ratio α_b for tension parallel to grain in ASTM is considered to be 0.55 times that for the bending, it is set to 0.55. This is because the wood tensile strength is more sensitive to defects such as knots and grain deviation than bending or compression strength (Doyle and Markwardt 1967).

3.4. Seasoning adjustment α_c

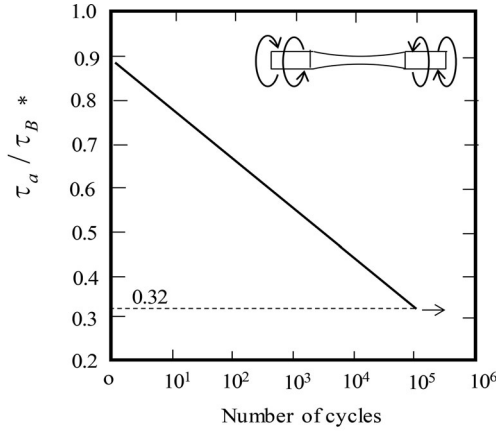
Seasoning adjustment α_c is a factor specified in ASTM D245, which takes the moisture content of wood into account. Since the moisture content of the JAS first-grade structural plywood is specified at 14% or less, i.e., dry state, seasoning adjustment α_c is not prescribed ($\alpha_c = 1.0$). The strength value for small clear wood specimens, which is used as a standard in ASTM D245, is in green condition. Wood strength increases when moisture content decreases. Thus, when the moisture content of wood actually used is low, the strength value must be increased ($\alpha_c > 1$). In ASTM, when the moisture content is 15% or less, the values of the lumber seasoning adjustment α_c are as follows: α_c for bending = 1.35, α_c for tension parallel to grain = 1.35, and α_c for compression parallel to grain = 1.75. However, this study uses the JAS first-grade structural plywood whose moisture content is 14% or less. The seasoning adjustment α_c for ASTM is therefore set to the same value as that for AIJ: $\alpha_c = 1.0$.

3.5. Environmental coefficient α_d

Environmental coefficient α_d is an AIJ coefficient that considers UV or wetting degradation of wood materials such as plywood with glue. Environmental coefficient α_d of plywood for the bending strength is shown as $\alpha_d = 3/4$. Environmental coefficient α_d for the compressive or tensile strength is shown as $\alpha_d = 6/7$. Environmental coefficient α_d for wood without glue is shown as $\alpha_d = 1.0$. Since ASTM specifies the lumber's strength evaluation method, it does not include this coefficient. This study adopts the same environmental coefficient α_d as AIJ.

3.6. Special factor α_e

According to Nakamura, Yamasaki, and Murata (2015), special factor α_e is a factor that reflects reductions in strength while the size of wood material is increased, based on the weakest-link theory (Bohannon 1966). More specifically, special factor α_e is a factor which is applied only to the bending strength. ASTM D245 uses it only for the bending strength of a material wider than 2 inches. This is prepared for beam members. The structural plywood used for sliding doors is out of scope. Therefore, in Table 1, special factor α_e is set to 1.0 both for ASTM and AIJ.



* τ_a / τ_B : Ratio of shear stress amplitude τ_a to shear strength τ_B

Figure 7. S-N curve of torsion fatigue test for Japanese beech.

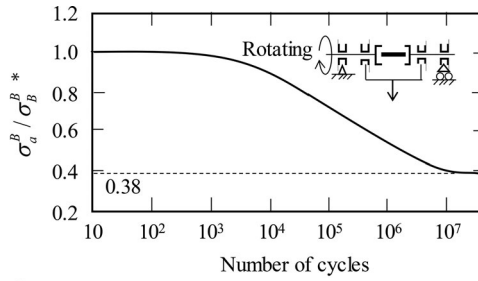
3.7. Product of coefficients α_f equivalent to ratio of fatigue limit to static strength σ_w/σ_B

The product of above-mentioned coefficients, $\alpha_a, \alpha_b, \alpha_c, \alpha_d,$ and $\alpha_e,$ is shown as "product of coefficients", $\alpha_f = \alpha_a \times \alpha_b \times \alpha_c \times \alpha_d \times \alpha_e,$ in [Table 1](#). The values of products of coefficients α_f derived from ASTM for structural plywood are as follows: α_f for tension = $0.21 < \alpha_f$ for bending = $0.34 < \alpha_f$ for compression = 0.43 . On the other hand, the corresponding AIJ values are as follows: α_f for bending = $0.25 < \alpha_f$ for tension and compression = 0.29 . The difference between ASTM and AIJ is caused by the following: AIJ does not differentiate between tensile strength and compression strength, and ASTM sets strength ratio α_b for tension for knots 0.55 times that for the bending. Comparing endurance ratios $\sigma_w/\sigma_B,$ these results indicate that taking the AIJ value $\sigma_w/\sigma_B^B = 0.25$ for bending, ASTM value $\sigma_w/\sigma_B^T = 0.21$ for tension, and AIJ value $\sigma_w/\sigma_B^C = 0.29$ for compression is safe.

In [Table 1](#), what is finally needed is $\alpha_f = \alpha_a \times \alpha_b \times \alpha_c \times \alpha_d \times \alpha_e,$ which is obtained by multiplying the coefficients. ASTM and AIJ show α_f just as "product of coefficient" and do not associate it directly with fatigue strength. From the viewpoint of the mechanical design, however, it is important to consider the fatigue strength under alternate loading. Therefore, the following discussion clarifies that the coefficient α_f is closely related to the endurance ratio $\sigma_w/\sigma_B,$ which is defined as the ratio of alternating fatigue limit σ_w to static strength σ_B for bending, tension and compression.

[Figure 6](#) shows the S-N curve of the three-point bending fatigue test for the Japanese sugi obtained by [Imayama and Matsumoto \(1970\)](#). The beam specimens are loaded at mid-span with a reversed and repeated point load at 40 cycles/second. The test specimens are made of mature 40-year-old sugi trunk logs with a water content of 12 to 15%. In [Fig. 6](#), the y-axis σ_a/σ_B shows the ratio of bending stress amplitude σ_a to bending strength $\sigma_B.$ [Figure 6](#) indicates the fatigue endurance ratio $\sigma_w/\sigma_B = 0.32$ at the number of cycles 10^7 for bending. The fatigue endurance ratio σ_w/σ_B is defined as the ratio of the fatigue limit σ_w to the static bending strength $\sigma_B.$

Another example is presented in [Fig. 7](#) ([Ando et al. 2005](#)), showing S-N curve for torsion fatigue test of Japanese beech. [Figure 7](#) indicates the fatigue endurance ratio $\tau_w/\tau_B = 0.32$ at the number of cycles 10^5 for torsion. Here, τ_w denotes the fatigue limit for torsion, and τ_B denotes the static torsion strength. Additionally, [Fig. 8](#) shows the S-N curve of the rotating fatigue test for Japanese cypress laminated wood obtained by [Maku and Sasaki \(1963\)](#). [Figure 8](#) indicates the fatigue endurance ratio $\sigma_w/\sigma_B = 0.38$ at the number of cycles 10^7 for rotating bending. Although



* σ_a^B / σ_B^B : Ratio of bending stress amplitude σ_a^B to bending strength σ_B^B

Figure 8. S-N curve of rotating bending fatigue test for Japanese cypress laminated lumber.

Table 2. Plywood material properties estimated from AIJ and ASTM used for FEM analysis.

Items	Plywood for door	
	ASTM	AIJ
Elastic modulus E	3.5 GPa	
Poisson's ratio ν	0.4	
Ultimate strength σ_B provided by AIJ		
	Bending σ_B^B	21.6 MPa
	Tension σ_B^B	11.9 MPa ^a (15.4 MPa) ^b
	Compression σ_B^C	8.7 MPa
Yield strength $\sigma_y = \sigma_B \times \alpha_{a2}$ (α_{a2} in Table 1)		
	Bending σ_y^B	17.2 MPa
	Tension σ_y^B	9.5 MPa (12.3 MPa) ^b
	Compression σ_y^C	7.6 MPa
Fatigue limit $\sigma_w = \sigma_B^T \times \alpha_f$ (α_f in Table 1)		
		2.5 MPa^c (3.2 MPa)^b
		3.4 MPa (4.4 MPa) ^b

^aStatic tensile strength σ_B^T in L-axis when the number of plates $N=7$ and plywood thickness $t_p = 15$ mm (see Table B2 in Appendix B) which are specified as first-grade C-C plywood by JAS (AIJ 2003, 2006).

^bHowever, as indicated in Table B2 in Appendix B, since AIJ values^a may have some misprints, presumed correct values are indicated in the parentheses.

^c**Bold numbers** denote the values recommended by the authors.

Okuyama, Itoh, and Marsoem (1984) investigated pulsating tension fatigue and pulsating compression fatigue in wood, they did not discuss fully reversed alternating tension-compression fatigue. From those studies mentioned above, the fatigue endurance ratio for alternating loading can be estimated as $\sigma_w / \sigma_B = 0.32$.

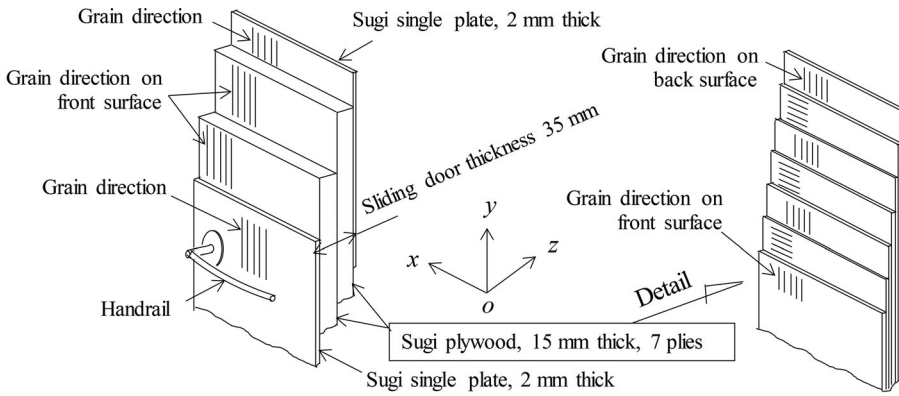
Products of coefficients α_f for ASTM and AIJ in Table 1 do not take load fluctuation into account. However, since product of coefficients for ASTM $\alpha_f = 0.21$ to 0.43 and that for AIJ is 0.25 to 0.29, it is determined that they correspond to the alternating fatigue limit endurance ratio shown in Figs. 6–8. In other words, products of coefficients α_f in Table 1 obtained in this section can be considered as the ratio of fatigue limit to static strength, σ_w / σ_B^T , σ_w / σ_B^C , and σ_w / σ_B^B .

4. Strength analysis of sliding door plywood part

This section examines the safety of the plywood part around the mounting plate of the sliding door shown in Fig. 1 using stress analysis. Since the strength of the attached mounting plate is designed according to the Japanese Industrial Standards (JIS A 1541-1:2016; JIS A 1513:1996), it is not studied here.

4.1. Mechanical properties of wood

Table 2 shows the mechanical properties of the sliding door materials required for the finite element method (FEM) analysis. The plywood material for the door shown in Table 2 where two



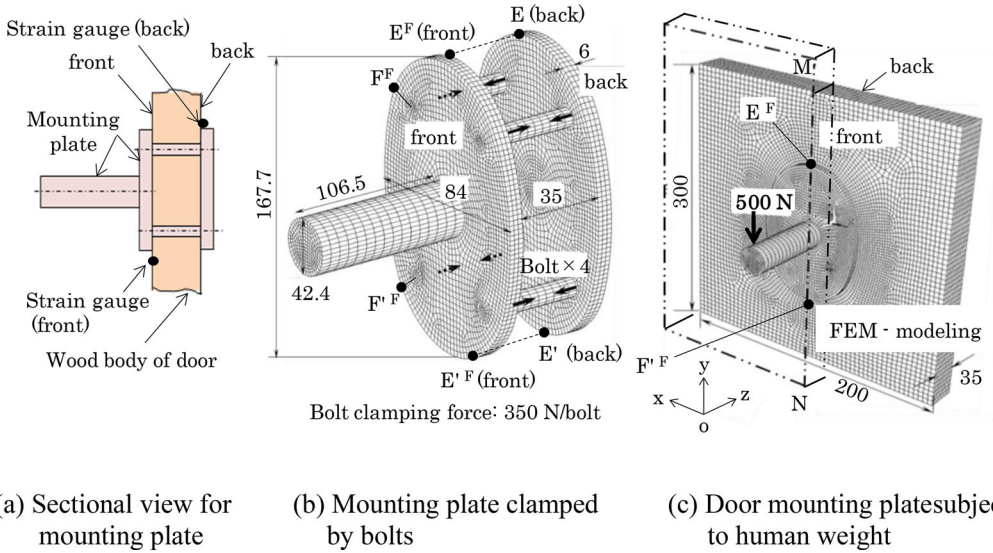
(a) Composition of sliding door material

(b) Composition of 15-mm thick plywood

Figure 9. Composition of sliding door material consisting of plywood boards.

cores 15 mm thick are bonded, and both front and back sides are covered with veneers 2 mm thick made of sugi, is used for the door on the whole. The total thickness of the sliding door is 35 mm including the thickness of the bonding agent. Figure 9 shows the composition of the door consisting of plywood boards. The strength of the sliding door plywood can be practically regarded as the strength of the core material. Based on tensile strength σ_B given for the first-grade structural plywood (C-C grade, sugi) in "Japanese agricultural standard for plywood" (JAS 2014), yield strength σ_y and fatigue limit σ_w for the sliding door plywood are shown in Table 2, using the plywood strength evaluation method for ASTM and AIJ described in Section 3. Since ASTM and AIJ do not describe the properties in the z-direction, Table 2 shows the properties in the x- and y-directions of the plywood. The tensile strength σ_B is the value for the first-grade structural plywood 15 mm thick (C-C grade, sugi) given in AIJ (2003). The tensile strength σ_B^T , that is, the ultimate strength under tension in Table 2 is considered as the most important property in mechanical design. In Table 2, σ_B^T is obtained from σ_B^L in L-axis = 11.9 MPa in Table B2. However, as indicated in Appendix B, since this AIJ value might be a misprint, the presumed correct value is also indicated in the parenthesis, although tensile strength $\sigma_B^T = 11.9$ MPa is on the safe side. The value in parallel direction to the front plate grain (JIS A 1541-1:2016), which shows a low stress value, is adopted. The yield strength is obtained by multiplying tensile strength σ_B^T by safety factor α_{a2} in Table 1. As shown in Appendix Fig. A5, the stress-strain diagram of structural plywood indicates that the endpoints of the test load are tensile strength σ_B^T , giving unclear yield strength σ_y . Since Table 2 shows that yield strength σ_y from AIJ is safer than that from ASTM for any of bending, tension, and compression, this study adopts the AIJ yield strength. The fatigue limit is obtained by multiplying tensile strength σ_B^T by product of coefficients α_f (in Table 1). Since the fatigue strength σ_w from ASTM is safer than that from AIJ, this study adopts the fatigue limit from ASTM.

As shown in Table B2 in Appendix B, the values for plywood strength ratio σ_B^T/σ_B^L are almost 1 except for the number of plates $N=3$ and $N=5$. Since plywood consisting of a larger number of plates becomes homogeneous, the plywood with $N=7$ plates or more can be considered as a homogeneous material. Although the plywood properties in the thickness direction may be different, no study is available. The plywood in this study is therefore determined to be an isotropic material. Young's modulus E in Table 2 is cited from the standard (JAS 2014). For the Poisson's ratio ν , the value at right angle to cross grain of the lauan plywood (Takami 1968) is used. Note that the scope of the strength study excludes veneers made of sugi.



(a) Sectional view for mounting plate

(b) Mounting plate clamped by bolts

(c) Door mounting plates subjected to human weight

Figure 10. FEM analysis model for mounting plate and door (unit: mm).

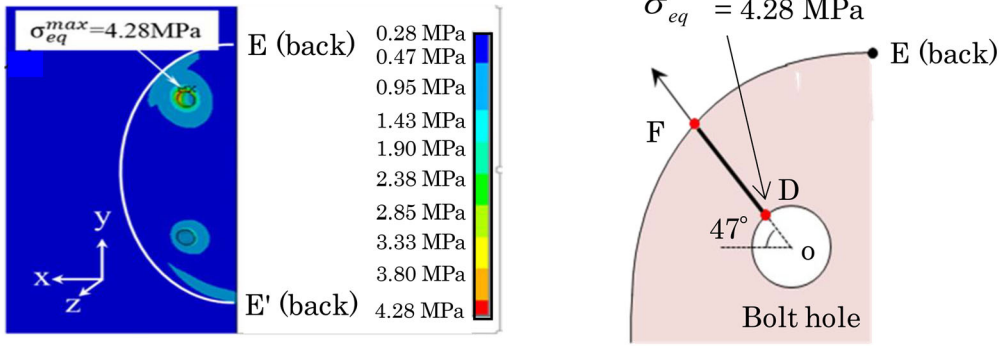
4.2. Method of stress analysis

Attention should be directed toward an area around the handrail bar mounting plate, which is the target of the analysis and assumed to be the most commonly damaged in operation. Figure 10 illustrates the FEM modeling for the mounting plate and door. Here, the mounting plate is fastened on the wooden plate by four bolts with the clamping force 350 N each. In this analysis, first, the bolt clamping force $350 \text{ N} \times 4$ is applied. Then, after the mounting plate is fixed to the door, the human supporting load 500 N is applied to the top of the mounting plate as shown in Fig. 10(c). According to an earlier study (Kato et al. 2004), the maximum support load is estimated at 500 N, which is used for this analysis. Considering the support load is fluctuating, although the bolt clamping force is constant, the strength of the wooden door will be investigated.

The geometry in Fig. 10(b) is designed by referring to bolt mounting on handles for wooden doors (JIS A 1541-1:2016). To increase the strength, each dimension in Fig. 10(b) has been scaled up to be bigger than common mounting plates for door knobs. The diameters of the mounting bolts are increased to M6 from M5 which is commonly used. Additionally, the number of bolts is doubled to four. The outline of the mounting plate is determined to be an oval figure in consideration of the limited space and strength of the mounting position to the door. The strength of the mounting plate used here satisfies the criteria for the strength test of parts mounting portions specified in the JIS (JIS A 1541-1:2016; JIS A 1513:1996). As will be seen in Section 5.1 and 5.3, the experiment proves no problems for the roller and rail at the end of the handrail bar as well as the mounting plate.

When the mounting plate to be installed on the sliding door plywood is fixed with the bolts, the plywood receives the compressive stress caused by the bolt clamping force in the direction of the board thickness. The clamping force is set to 350 N so that the compressive stress during installation is one sixth of the plywood yield strength (safety factor of 3).

To confirm the safety of the entire door, the analysis target is narrowed to the wooden part of $200 \text{ mm} \times 300 \text{ mm} \times 35 \text{ mm}$ centered around the plate. Furthermore, as shown in the two-dotted line in Fig. 10(c), a half model can be used because of its symmetry both in geometry and load. The total number of elements is 83068 and the total number of nodes is 83202. Using



(a) Stress distribution

(b) Position of maximum stress

Figure 11. Equivalent stress on back side (see Fig. 10) under action of bolt clamping and human weight 500 N.

commercially available ANSYS WORKBENCH 16.2 for the analysis code, a non-linear analysis is conducted in consideration of elastic contact. As shown in Fig. 10(a) to (c), although the modeling of the metal part and the wood part are carried out separately, the contact between the two parts is considered in the meshing of the two parts, and the mesh grids are completely corresponding in the front-rear direction. The mesh density is controlled so that any part of the structure has at least four layers of node in the direction of the minimum thickness. The contact surface between metal and wood is a rough surface without polishing, and the friction coefficient measured in the experiment is 0.5. Prior to the analysis, strains of the sliding door around the mounting plate are measured with gauges on both front and back sides. Details will be described in Section 5.3. For the back side which received a greater strain amplitude in measurement, the results are shown in Section 4.3.

4.3. Static strength evaluation based on the maximum stress

First, this section provides a consideration assuming "one-shot" destruction caused by the maximum stress. Figure 11 shows the equivalent stress based on the FEM analysis results on the back side of the door board around the bolt mounting plate fixed area, which has the highest risk of destruction. Figure 11(a) is a perspective view from the front side, which shows the stress distribution on the back side when the support load of 500 N is applied after the mounting plate is tightened with the bolts as shown in Figs. 11(b), 10(b), and (c).

As shown in Fig. 11(a) and (b), the maximum equivalent stress is generated at point D around the bolt hole. Thus, Fig. 12 shows the distribution of the stress generated along line DF (Fig. 11(b)) from point D around the hole (starting point), including the principal stresses of σ_1 , σ_2 , and $\sigma_3 = \sigma_z$ which can be used for the fatigue strength evaluation of the board. Adding the support load of 500 N changes the stress with the bolts tightened, as shown in Fig. 12(a) and (b). In Fig. 12(b), the maximum compressive principal stress is shown as $\sigma_3 = -3.95 \text{ MPa}$, which is generated around the bolt hole at the topside of the back side. On the other hand, the maximum tensile principal stress is shown as $\sigma_1 = 0.85 \text{ MPa}$. The maximum compressive and tensile stresses act at point D.

In Table 3, attention should be firstly directed toward the maximum tensile stress $\sigma_1 = 0.85 \text{ MPa}$ and the maximum compressive stress $\sigma_3 = -3.95 \text{ MPa}$ around the hole. It summarizes how safe they are against tensile yield strength σ_y^T and compressive yield strength σ_y^C in Table 2 by defining the safety factor $= \sigma_y^T / \sigma_{\max}^T$ and safety factor $= \sigma_y^C / \sigma_{\max}^C$. According to Table 3, safety

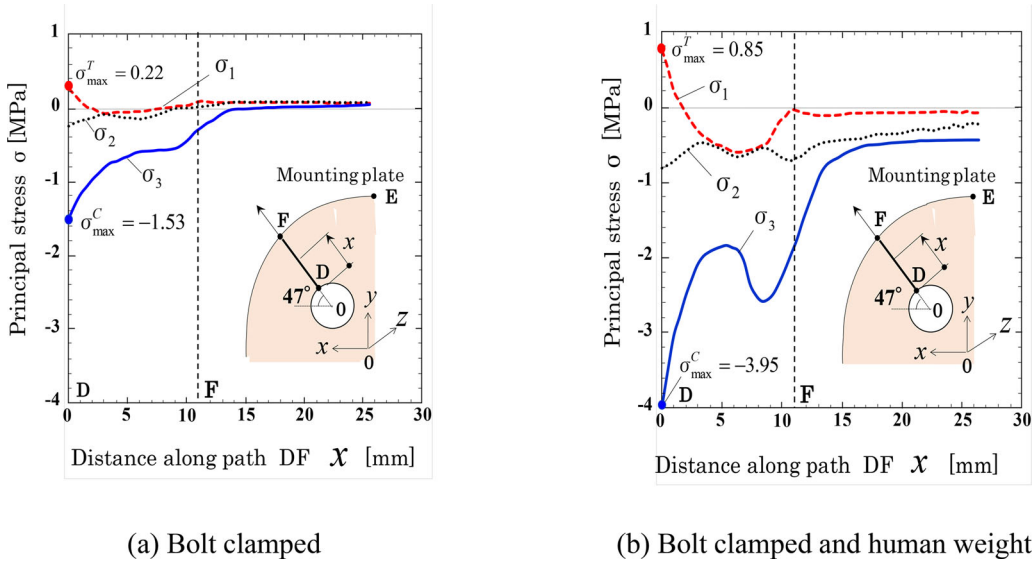


Figure 12. Principal stress distribution along path DF (back side).

Table 3. Maximum stress, yield strength, and safety factor at point D in Fig. 11(b).

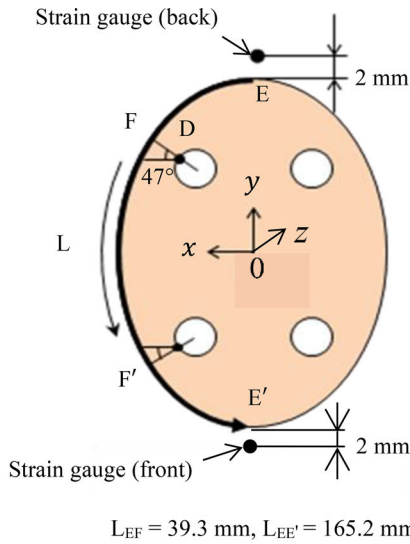
Maximum stress in Fig. 12(b)	Yield strength in Table 1	Safety factor
Maximum tensile stress $\sigma_{\max}^T = 0.85$ MPa	$\sigma_y^T = 7.8$ MPa (AlJ)	$\sigma_y^T / \sigma_{\max}^T = 9.1$
Maximum compressive stress $\sigma_{\max}^C = -3.95$ MPa	$\sigma_y^C = 5.8$ MPa (AlJ)	$\sigma_y^C / \sigma_{\max}^C = 1.4$

factor $\sigma_y^T / \sigma_{\max}^T = 9.1$ (tensile yield strength σ_y^T to the maximum tensile stress σ_{\max}^T) indicates adequate safety. Meanwhile, the safety factor of compressive yield strength σ_y^C to the maximum compressive stress σ_{\max}^C is shown as $\sigma_y^C / \sigma_{\max}^C = 1.4$. Furthermore, the safety factor against compressive strength σ_B^C is shown as $\sigma_B^C / \sigma_{\max}^C = 2.2$, providing adequate safety. However, since there are concerns, which include a possible chip around the bolt holes where the generated maximum compressive stress focuses, the safety will be confirmed by the repeated load test in Section 5.

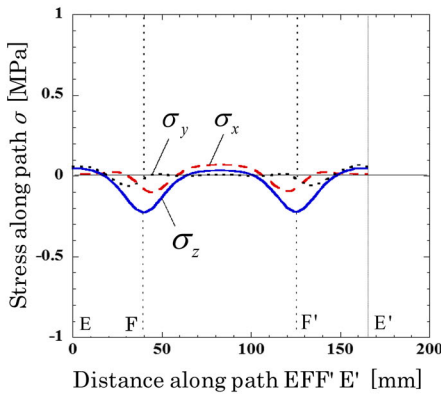
Figure 13 which focuses on the possibility of damage around the mounting plate shows the distribution of the stress generated on the back side of the door board. Adding the support load of 500 N changes the stress with the bolts tightened, as shown in Fig. 13(b) and (c). In Fig. 13(b), the compressive stress is generated around point F and point F' near the bolt holes in the direction of the board thickness, which is caused by the tightened bolts. As shown in Fig. 13(c), adding the support load of 500 N on the mounting plate increases compressive stress σ_z at point F from -0.25 MPa to -0.76 MPa. The maximum tensile stress $\sigma_y = 0.95$ is also generated around point E' (back). These results attract attention to point E (back) shown in Fig. 10(b), the mounting plate head part on the back side of the sliding door where the maximum stress is generated, as well as point E'F (front), the mounting plate bottom part where the maximum stress is generated on the front side. More specifically, strain gauges are attached at points (see Fig. 13(a)) 2 mm separated from the mounting plate edges of point E'F (front) and point E (back). At these 2 points, the strain changes caused by the repeated support load are monitored. Section 5.3 will discuss the results.

4.4. Strength evaluation for fatigue based on stress amplitude

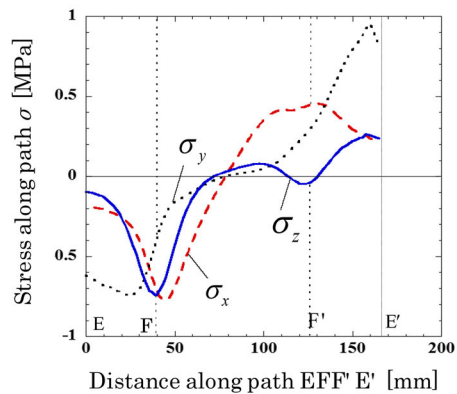
Table 4 summarizes the stress amplitude σ_a and average stress σ_m based on common view in metal fatigue. The metal fatigue strength is usually evaluated from the stress amplitude σ_a and



(a) Path EFF'E' along mounting plate edge



(b) Stress due to clamped bolt



(c) Stress due to clamped bolt and human weight

Figure 13. Stress distribution along path EFF'E' on back side in Fig. 10(b).

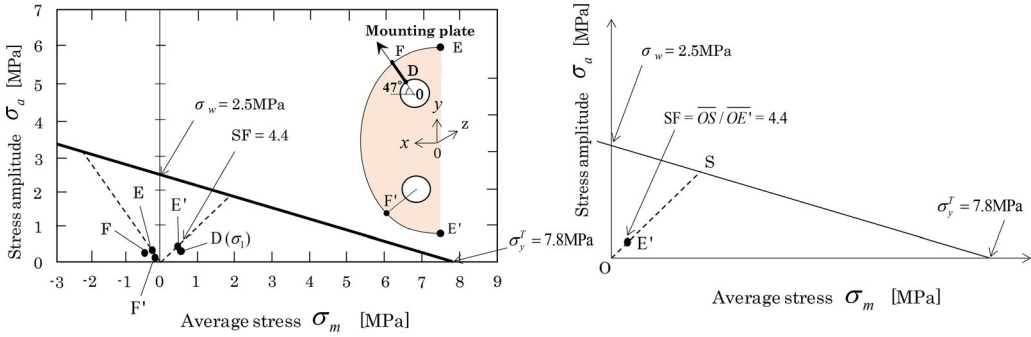
the average stress σ_m (Ishibashi 1969). This is because the stress amplitude σ_m controls crack initiation and the average stress σ_m controls crack propagation. By comparing Fig. 12(a) and (b), σ_a and σ_m are obtained; then, Table 4 shows the high-risk point D at the bolt hole edge. By comparing Fig. 13(a) and (b), σ_a and σ_m are obtained; then, Table 4 also shows the high-risk points E and F at the mounting plate edges. In Figure 14, the results in Table 4 are plotted on the endurance limit diagram.

As described in Section 4.1, the plywood can be considered to be isotropic in the x- and y-directions (see Fig. 9) although the z-direction may have different properties. Recently, Kuwamura (2010) also clarified that plywood is isotropic in the x- and y-directions but no study is found for the z-direction. In this FEM analysis, therefore, the same material properties are

Table 4. Average stress σ_m and stress amplitude σ_a along mounting plate edge in Fig. 13(a).

Position	Stress component	σ_m [MPa]	σ_a [MPa]	Safety factor SF (from Fig. 14)
D in Fig. 12(a), (b)	σ_1	0.54	0.32	5.1 (6.5) ^a
E in Fig. 13(b), (c)	σ_y	-0.28	0.34	10.0
F in Fig. 13(b), (c)	σ_z	-0.49	0.26	24.5
F' in Fig. 13(b), (c)	σ_z	-0.15	0.1	48.2
E' in Fig. 13(b), (c)	σ_y	0.50	0.45	4.4 (5.7)*

^aThe safety factor SF = 5.1 and SF = 4.4 are obtained in Fig. 14 based on $\sigma_B^T = 11.9$ MPa, $\sigma_y^T = 7.8$ MPa, $\sigma_w = 2.5$ MPa, which are obtained from $\sigma_B^L = 11.9$ MPa in Table B2, which may be a misprint in JAS (AIJ 2003, 2006). If $\sigma_B^T = 15.4$ MPa is correct, σ_y^T and σ_w become 1.3 times larger. Then, presumed correct SF values are indicated in parentheses.



(a) Endurance limit diagram

(b) Definition of safety factor SF

Figure 14. Endurance limit diagram based on $\sigma_B^T = 11.9$ MPa, $\sigma_y^T = 7.8$ MPa and $\sigma_w = 2.5$ MPa in Table 2 with the definition of safety factor SF. Note that $\sigma_B^L = 11.9$ MPa is estimated from $\sigma_B^T = 11.9$ MPa in Table B2, which may be a misprint in JAS (AIJ 2003, 2006) as described in Appendix B. If $\sigma_B^T = 15.4$ MPa is correct, σ_y^T and σ_w become 1.3 times larger.

assumed in the z-direction. As shown in Table 4, the critical points in terms of fatigue are stresses in the x-y plane, and the stress amplitude of σ_z is relatively small. To provide the safest condition, the fatigue strength is verified based on fatigue limit stress σ_w and yield stress σ_y . All of these five points are within the range of the endurance limit line, being shown to be safe in strength. The safety factors SF = 5.1 and SF = 4.4 are obtained in Fig. 14 based on $\sigma_B^T = 11.9$ MPa, $\sigma_y^T = 7.8$ MPa, $\sigma_w = 2.5$ MPa, which are obtained from $\sigma_B^L = 11.9$ MPa in Table B2, which may be a misprint in JAS (AIJ 2003, 2006). If $\sigma_B^T = 15.4$ MPa is correct, σ_y^T and σ_w become 1.3 times larger. Then, presumed correct SF values are indicated in parentheses.

5. Experimental study on endurance of sliding door

The previous section indicates that there is a concern about a possible chip around the bolt holes regarding the compressive stress while the maximum tensile stress has adequate safety according to Table 3. Hence, in this section, a repeated opening-closing test of the door and a repeated load test on the mounting plate are conducted using the prototype door. In the opening-closing test, the structural parts including the rail and rollers are checked for damage. In the load test, the fluctuation of the strain against the repeated load, which is generated on the front and back side of the door, as well as dents generated around the mounting plate and deformation of the door surface are measured. Prior to the experiment, a pilot study has revealed that the damage caused by the repeated load around the mounting plate can be evaluated by an increase of the strain.

5.1. Methods and results of repeated opening-closing test

A reciprocating operation from the closed state to opened state of the sliding door is regarded as one time. After 2×10^5 times, the structural parts including the rail and rollers are checked for damage with visual inspection and dye flaw detection. At the same time, warpage and deformation of the door is measured. The repeated opening-closing test of 2×10^5 times brought the following results: (1) no abnormal deformation of the handrail, (2) no wear or abnormal deformation of the guide rail, (3) no wear of the rollers or abnormal deformation of the roller axes without unusual noise during the test operation, and (4) 0.8 mm door warpage or less, which did not affect the opening-closing usage of the sliding door and satisfies the requirements specified in "Windows and doorsets—General rule for test method" (JIS A 1513:1996) and "Windows and door—Resistance to repeated opening and closing—Test method" (JIS A 1530:2014). In addition, no deformation of the wheels at the bottom of the door or unusual noise during operation was found.

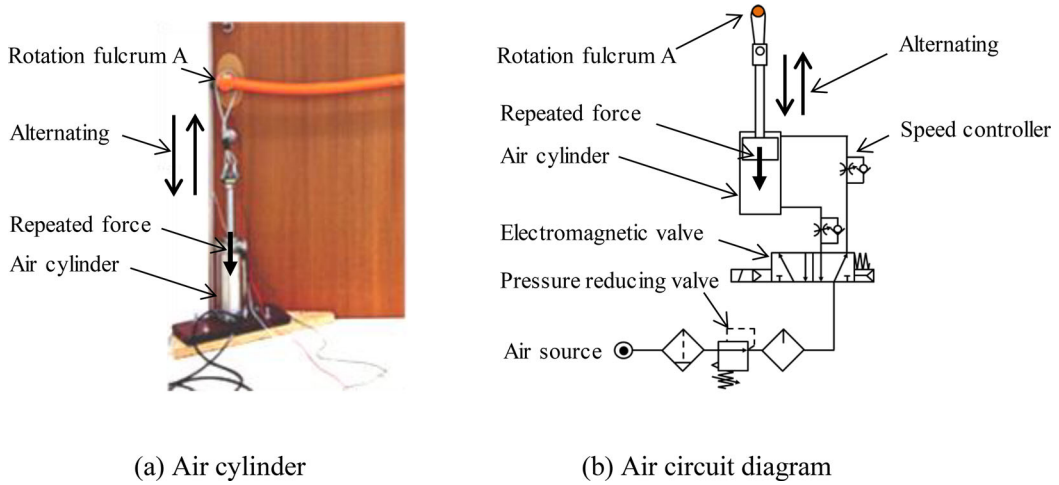
5.2. Methods of repeated load test

The fluctuation of the strain generated on the front and back side of the door by the maximum compressive stress is monitored while it is used repeatedly. The fluctuation is studied along with the number of repeated operations. It is considered that a significant damage due to fatigue changes the corresponding strain. For this purpose, based on the analysis results in the previous section, the strain gauges are attached at the points 2 mm separated from the mounting plate edges of point E (back) and point EF (front) shown in Fig. 10(b). See Fig. 13(a) for details. Since plywood consisting of a larger number of plates becomes homogeneous, the plywood with 7 plates or more can be considered as a homogeneous material. It is known that the difference between the strains detected on the surface and central layers is 2 to 3%. The support load of 500 N is vertically and repeatedly added at the tip of the fulcrum axis of the mounting plate shown in Figure 10, using an air cylinder. This load is a pulsating load (stress ratio $R=0$). The plywood in the area where the mounting plate is attached is checked to see if it withstands the designed target for repeated load, 2×10^5 times. This number of repeated operations is twice as many times as the allowable number of uses of sliding doors specified in the requirement (1×10^5 times, JIS A 4702:2000) and more than twice as many times as that of aluminum window sashes specified in the requirement (3×10^4 times, JIS A 4706:2000).

Figure 15(a) shows the air cylinder device which applies a load. In Fig. 15(a), the load of the air cylinder is directly applied at the tip of the fulcrum axis so as to maximize the load on the mounting plate. Figure 15(b) shows the air circuit diagram. The internal diameter and the stroke of the air cylinder used are φ 40 mm and 140 mm, respectively. The tip of the air cylinder and the handrail position of the mounting plate are tied with a wire rope of φ 6 mm. The pulling-side operation of the air cylinder adds a load on the mounting plate. The compressor air pressure is set to 0.47 MPa with a pressure reducing valve so that the cylinder applies the load at 500 N. Switching of pulling pressure operation is controlled with a timer of an electromagnetic valve. In this experiment, the repeating speed is set to 3.8 seconds/time. The strain of the sliding door surface due to the load is measured with the strain gauges attached around the top and bottom end of the mounting plate on the front and back side of the sliding door. The repeated operations are counted with a mechanical counter. Details are shown in Fig. 15(b).

5.3. Results of repeated load test

Figure 16 shows the result of the fatigue test using the actual door: the strain on the board front surface ε_y (E'F [front]) and that on the back surface ε_y (E [back]). No significant change or



(a) Air cylinder

(b) Air circuit diagram

Figure 15. Fatigue test equipment.

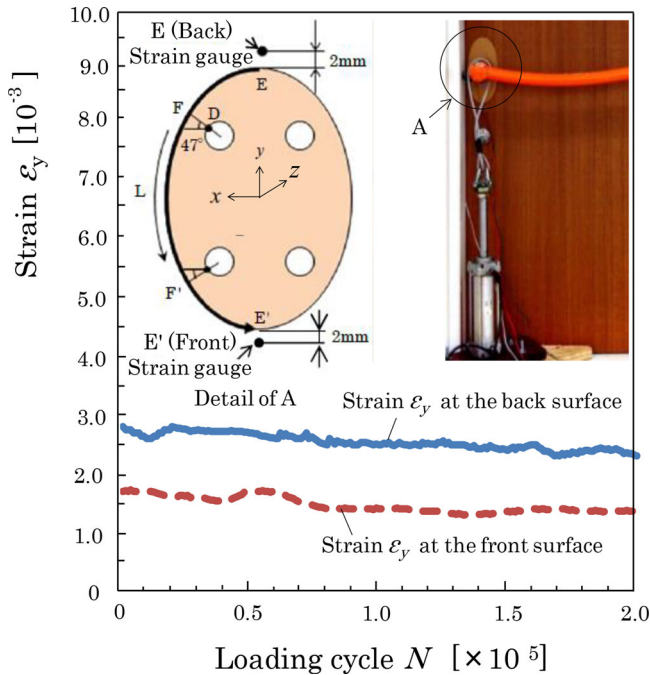


Figure 16. Strain versus loading cycle.

damage was found on the strain of both sides even after 2×10^5 times of the repeated operations. The difference between the strains on the front and back side includes the effects of works attaching the strain gauges with bonding agents, board surface roughness, and uneven board fibers.

After the experiment was completed, the area around the bolt holes of the board at the bottom of the mounting plate was visually checked for cracks. The holes are found to be slightly chipped, and the chipped areas are approximately 1 mm long. They are considered to be generated while the holes were made. There is no visible crack around the areas. Additionally, as shown in Fig. 17(a), the front surface profile was measured with the mounting plate installed area at the center using a dial gauge to observe change on the front surface shape. First, the back side of the sliding

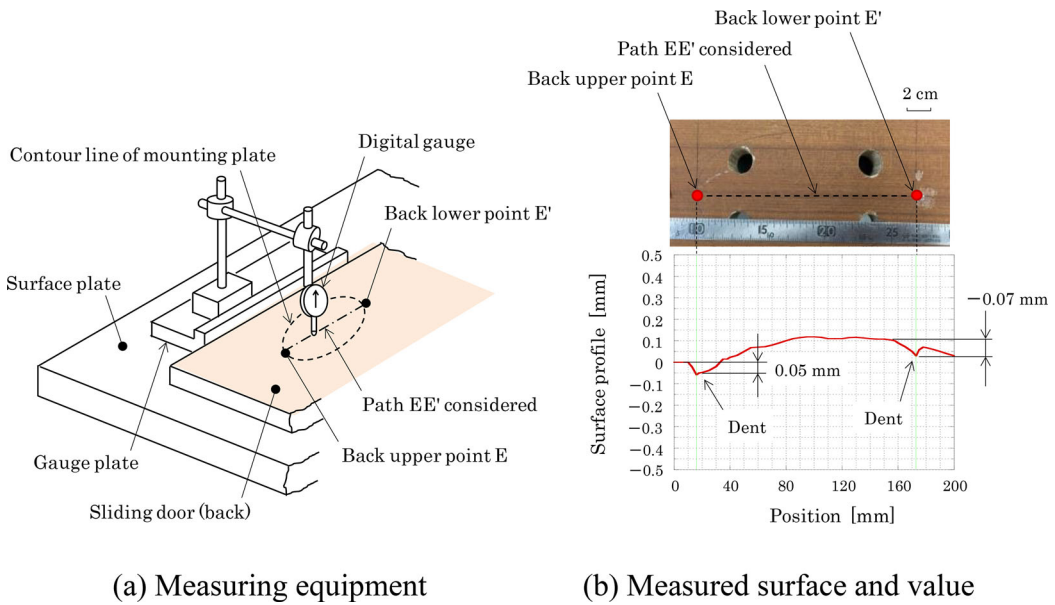


Figure 17. Measuring strain after repeated loading.

door was placed in an upward and horizontal position and fixed on the surface plate. Next, a gauge plate was set in parallel with the edge along the length of the sliding door, the dial gauge block was moved along the gauge plate, and the door front surface profile was measured with the digital dial gauge including the mounting plate installed area. Figure 17(b) shows the measurement results. Two impressions, -0.05 mm and -0.07 mm, were detected at the top and bottom edges of the plate installed position, which do not affect the strength. For the concern about a possible chip around the bolt holes, no damage that has a controversial impact was found. The warpage of the door surface caused by the repeated load test was 0.8 mm at the maximum. The mounting plate after the opening/closing test did not show any deformation.

Since the door is made of plywood, shrinkage/swelling due to moisture variations can cause looseness or backlash. Obviously, as a countermeasure, it is necessary to use sufficiently dried boards and to perform maintenance including retightening required for shrinkage.

6. Conclusion

The sliding door with the retractable handrail examined in this study can be installed in hospitals and nursing facilities for helping the elderly and disabled to walk independently. Preventing a decline in walking ability has been confirmed to help maintain and restore ability. Since wood is used as mechanical structural parts in this product development, the strength evaluation is required. However, there is no clear standard for the wood fatigue. Hence, this study shows the method of calculating the yield strength and fatigue limit of structural plywood used in this study by investigating the methods of obtaining allowable stresses in ASTM and AIJ, which are intended to be used for building construction. The following describes the conclusions.

1. The methods of calculating allowable stresses were investigated in ASTM and AIJ, which are intended to be used for building construction. When the plywood yield stresses are estimated, AIJ provides the safer evaluation than ASTM. Consequently, tensile yield stress $\sigma_y^T =$

7.8 MPa and compressive yield stress $\sigma_y^C = 5.8$ MPa are obtained for the structural plywood used in this study.

2. Using the FEM analysis, the maximum stress σ_{\max}^T was calculated on the area around the handrail bar mounting plate where the highest risk is assumed. The result indicates that the maximum tensile stress σ_{\max}^T is less than tensile yield stress σ_y^T , $\sigma_{\max}^T = 0.85$ MPa $<$ $\sigma_y^T = 7.8$ MPa, and safety factor is $\sigma_y^T/\sigma_{\max}^T = 9.1$. It also indicates that the maximum compressive stress σ_{\max}^C is less than compressive yield stress σ_y^C , $\sigma_{\max}^C = 3.95 < \sigma_y^C = 5.8$ MPa, and safety factor is $\sigma_y^C/\sigma_{\max}^C = 1.4$. Adequate safety was confirmed to be provided.
3. Investigating calculation method of wood strength in ASTM and AIJ reveals that product of coefficients α_f equals the ratio of fatigue limit to static strength σ_w/σ_B , i.e., endurance ratio. The investigation results show that ASTM provides the safer evaluation than AIJ, contrary to the case of the yield stress. Furthermore, the maximum stress amplitude and average stress were determined on the area around the handrail bar mounting plate and examined on the endurance limit diagram. The results are within the range of the endurance limit line connecting tensile yield stress σ_y^T and alternating fatigue limit σ_w , being shown to be safe in fatigue strength.
4. The fatigue test on the prototype sliding door was conducted where the load of 500 N was repeatedly applied on the mounting plate 2×10^5 times. The number is more than that specified in the JIS standards. Checking the sliding door after the fatigue test revealed that there was no damage around the bolt holes on the mounting plate where there was a concern. It was confirmed to have sufficient strength. Additionally, in the repeated opening-closing test, no damage that can affect the use was generated. The results on both tests satisfy the requirements specified in "Windows and doorsets—General rule for test method" (JIS A 1513:1996).

Nomenclature

$F_{Ax}(x_A)$	Opening force applied at point A in Figure A2 . Target value $F_{Ax}(x_A) = 19.6$ N
$F_{Ay}(x_A)$	Reaction force applied to handrail at point A $(x_A, 0)$ in y-direction in Figure A2
$(x_{A0}, y_{A0}) = (x_A, 0)$	Coordinates of supporting point A in Figure A1 , $x_A =$ Opening distance of sliding door
(x_{B0}, y_{B0})	Coordinates of point B in Figure A1 , Point B = Center of guide roller
(x_D, y_D)	Coordinates of point D in Figure A1 , Point D = Center of arc portion of guide rail
Q	$Q = \mu_t P$, Running resistance (see Figure A2)
P	Reaction force to handrail from guide rail at point B in Figure A2
R	Rolling surface radius of guide rail stand in Figure A1 ($R = 478$ mm, for prototype)
θ	Angle between retractable handrail and horizontal line (see Figure A1)
φ	Handrail angle between tangential direction of guiderail at B and handrail (see Figure A1)
ε	Guide rail angle between tangential direction of guiderail and vertical direction (see Figure A1)
W	Weight of handrail including guide roller in Figure A2 ($W = 13.7$ N, for prototype steel handrail)
M	Moment due to assist device in Figure A2 ($M = k(0.5\pi - \theta)$)
k	Assist device spring constant
μ_t	Friction coefficient of bearing 0.03 + friction coefficient of rotating roller 0.005 in Figure A2 ($\mu_t = 0.03 + 0.005 = 0.035$)
a	$a = y_A - y_{B0}$, AB in y-direction in Figure A1 ($a = 22.6$ mm, for prototype)
b	Horizontal difference, $b = x_A - x_{B0}$, between point A and point B in Figure A1 ($b = 910.3$ mm, for prototype)
c	Distance in x-direction from guide roller contact point to rail vertical point in Figure A1
r	Radius of guide roller B in Figure A1 ($r = 17.5$ mm for prototype)
e	Distance in x-direction between center point of guide roller B and contact point of roller and rail in Figure A1
l	Length of retractable handrail rod in Figure A1 ($l = 910.3$ mm for prototype)
C	Contact point of roller in Figure A1
E	End point of curved portion of guide rail in Figure A1
F	Guide rail end in Figure A1

References

- Ando, K., M. Yamasaki, J. Watanabe, and Y. Sasaki. 2005. Torsional fatigue properties of wood. *Mokuzai Gakkaishi* 51 (2):98–103. doi:10.2488/jwrs.51.98.
- AIJ (Architectural Institute of Japan). 2003. *Recommendation for limit state design of timber structures (draft)*. 369 vols. Tokyo: Maruzen.
- AIJ (Architectural Institute of Japan). 2006. *Standard for structural design of timber structures*, 149–60. 408 vols. Tokyo: Maruzen.
- Arfken, C. L., H. W. Lach, S. J. Birge, and J. P. Miller. 1994. The prevalence and correlates of fear of falling in elderly persons living in the community. *American Journal of Public Health* 84 (4):565–70.
- ASTM D245-06(2019). 2019. *Standard practice for establishing structural grades and related allowable properties for visually graded lumber*. West Conshohocken, PA: ASTM International.
- ASTM D2555-17a. 2017. *Standard practice for establishing clear wood strength values*. West Conshohocken, PA: ASTM International.
- Bedon, C., C. Amadio, and S. Noè. 2019. Safety issues in the seismic design of secondary frameless glass structures. *Safety* 5 (4):80. doi:10.3390/safety5040080.
- Bohannon, B. 1966. *Effect of size on bending strength of wood members*. Research Paper FPL 56:2–18. Madison, WI: Department of Agriculture, Forest Service, Forest Products Laboratory.
- Chu, L.-W., C. K. W. Pei, A. Chiu, K. Liu, M. M. Chu, S. Wong, and A. Wong. 1999. Risk factors for falls in hospitalized older medical patients. *Journal of Gerontology: Series A* 54 (1):M38–43.
- Cumming, G. R., G. Salkeld, M. Thomas, and G. Szonyi. 2000. Prospective study of the impact of fear of falling on activities of daily living, SF-36 scores, and nursing home admission. *Journal of Gerontology: Series A* 55 (5): M299–305.
- Doyle, D. V., and L. J. Markwardt. 1967. Tension parallel-to-grain properties of southern pine dimension lumber. *Research Paper FPL 84:8–10*. Madison: Department of Agriculture, Forest Service, Forest Products Laboratory.
- Gault, M. L., and M. E. Willems. 2013. Aging, functional capacity and eccentric exercise training. *Aging and Disease* 4 (6):351–63.
- Gunter, K. B., K. N. White, W. C. Hayes, and C. M. Snow. 2000. Functional mobility discriminates nonfallers from one-time and frequent fallers. *Journal of Gerontology: Series A* 55 (11):M672–76.
- Howland, J., M. E. Lachman, E. W. Peterson, J. Cote, L. Kasten, and A. Jette. 1998. Covariates of fear of falling and associated activity curtailment. *The Gerontologist* 38 (5):549–55.
- Imayama, N., and T. Matsumoto. 1970. Studies on the fatigue of wood. I: Phenomenal study on the fatigue process. *Mokuzai Gakkaishi* 16 (7):319–25.
- Ishibashi, T. 1969. *Kinzoku no hirou to hakai no boushi [Prevention of metal fatigue and destruction]*. 11:1. Tokyo: Yokendo.
- JAS (Japanese Agricultural Standard). 2014. *JAS for Plywood. Notification No. 303. February 25, 2014*. Tokyo: Ministry of Agriculture, Forestry and Fisheries.
- JIS A 1513. 1996. *Windows and doorsets—General rule for test method*. Tokyo: Japanese Industrial Standards Committee.
- JIS A 1530. 2014. *Windows and door—Resistance to repeated opening and closing—Test method*. Tokyo: Japanese Industrial Standards Committee.
- JIS A 1541-1. 2016. *Building hardware—Locks and latches— Part 1: Test methods for locks and latches*. Tokyo: Japanese Industrial Standards Committee.
- JIS A 4702. 2000. *Doorsets*. Tokyo: Japanese Industrial Standards Committee.
- JIS A 4706. 2000. *Windows*. Tokyo: Japanese Industrial Standards Committee.
- Kato, M., T. Yatogo, K. Nomura, K. Nunota, and H. Naoi. 2004. Classification of handrails from the viewpoint of human action and measurement of human force applied to handrails during accidental tumbling: Experimental study on the strength evaluation method of installed handrails on wall in dwellings (1). *Journal of Architecture and Planning* 584:27–33.
- Kim, H., H. Yoshida, T. Suzuki, T. Ishizaki, T. Hosoi, A. Yamamoto, and H. Orimo. 2001. The relationship between fall-related activity restriction and functional fitness in elderly women. *Nihon Ronen Igakkai Zasshi. Japanese Journal of Geriatrics* 38 (6):805–11.
- Kubo, Y. 2010. Handrail for sliding door, sliding door device. Japan Patent 4,639,358, filed April 27, 2010, and issued December 10, 2010.
- Kubo, Y. 2017. Handrail for sliding door, sliding door device. Japan Patent 6,174,304, filed June 13, 2012, and issued July 14, 2017.
- Kuwamura, H. 2010. Anisotropic elasticity and strength in in-plane behavior of plywood: Study on steel-framed timber structures Part 7. *Journal of Structural and Construction Engineering (Transactions of AIJ)* 75 (653):1317–26. doi:10.3130/aijs.75.1317.

- Lachman, M. E., J. Howland, S. Tennstedt, A. Jette, S. Assmann, and E. W. Peterson. 1998. Fear of falling and activity restriction: The survey of activities and fear of falling in the elderly. *Journal of Gerontology: Series B* 53 (1):43–50.
- Maku, T., and H. Sasaki. 1963. The rotating bending fatigue strength of glued laminated wood. Kyoto: Wood Research: Bulletin of the Wood Research Institute, Kyoto University, 31, 1–10.
- Nakamura, N., M. Yamasaki, and K. Murata. 2015. *Timba Mekanikusu—Mokuzai no rikigaku riron to oyo [Timber mechanics: Theory and applications]*. 130–5. Otsu: Kaiseisha.
- Okuyama, T., A. Itoh, and S. N. Marsoem. 1984. Mechanical responses of wood to repeated loading. I: Tensile and compressive fatigue fractures. *Mokuzai Gakkaishi* 30 (10):791–8.
- Porter, M. M., A. A. Vandervoort, and J. Lexell. 1995. Aging of human muscle: Structure, function and adaptability. *Scandinavian journal of Medicine & Science in Sports* 5 (3):129–42. doi:10.1111/j.1600-0838.1995.tb00026.x.
- Saitou, K., N.-A. Noda, Y. Sano, Y. Takase, K. Murai, Z. Wang, S. Li, X. Liu, H. Tanaka, and Y. Kubo. 2018. Special sliding door with storable handrail to support senior and handicapped persons to walk by themselves. *IOP Conference Series: Materials Science and Engineering* 372 (012009):012009–6. doi:10.1088/1757-899X/372/1/012009.
- Saitou, K., N.-A. Noda, Y. Sano, Y. Takase, K. Murai, Z. Wang, S. Li, X. Liu, H. Tanaka, and Y. Kubo. 2021. Semi-automatic retractable handrail utilizing opening/closing movement of sliding door supporting elderly people to walk independently. *Accessibility and Design for All* 11 (1):1–19.
- Sawada, M. 1959. *Mokuzai no kyodo tokusei ni kansuru kenkyu, shutosite sono mokuzai hari eno tekiyo* [Study on strength properties of wood: Application for timber beam]. *Japanese Forest Society* 41:118–31.
- Takami, I. 1968. *Gohan no tsuyosa ni tsuite (I)* [Strength of plywood (I)]. *Bulletin of the Government Forestry Experiment Station* 208:1–27.
- Wood, L. W. 1951. *Relation of strength of wood to duration of load*. Report No. 1916. 1–9. Madison: Department of Agriculture, Forest Service, Forest Products Laboratory.
- World Health Organization. 2007. WHO global report on falls prevention in older age. 1–19. Accessed March 16, 2021. <https://extranet.who.int/agefriendlyworld/wp-content/uploads/2014/06/WHO-Global-report-on-falls-prevention-in-older-age.pdf>

Appendix A: Analysis of sliding door opening force

A1: Notations

The following notations are used in this paper.

A2: Equilibrium of handrail to obtain opening force

Figure A1 shows the handrail model to be considered where no assist device is assumed to be installed to the rotation fulcrum shaft. Figure A2 shows the free body diagram for the handrail where an assist device is installed to the rotation fulcrum shaft. Equations (A1) to (A3) are derived from the equilibrium shown in Fig. A2.

$$F_{Ax}(x_A) = Q\cos(\theta + \phi) + P\sin(\theta + \phi) \quad (\text{A1})$$

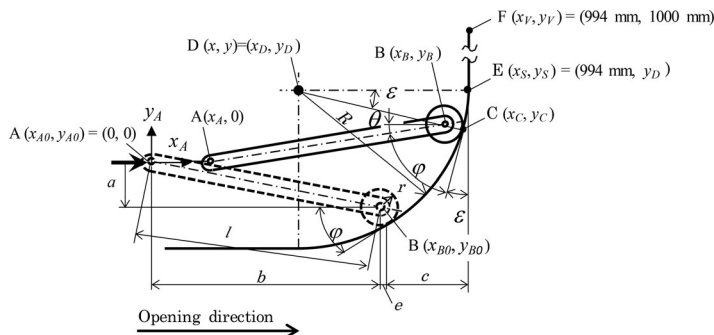


Figure A1. Model of retractable handrail.

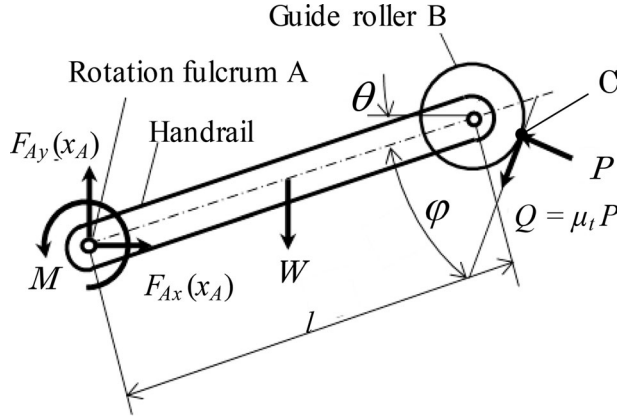


Figure A2. Equilibrium of force with assist device.

$$F_{Ay}(x_A) + P\cos(\theta + \phi) = W + Q\sin(\theta + \phi) \quad (\text{A2})$$

$$M + lP\cos\phi = \frac{1}{2}lW\cos\theta + lQ\sin\phi \quad (\text{A3})$$

From equations (1) to (3), the following expressions can be obtained.

$$F_{Ax}(x_A) = \mu_t P\cos(\theta + \phi) + P\sin(\theta + \phi) \quad (\text{A4})$$

$$F_{Ay}(x_A) = W + \mu_t P\sin(\theta + \phi) - P\cos(\theta + \phi) \quad (\text{A5})$$

As shown in Fig. A1, a Cartesian coordinate system (x, y) is used to describe the handrail position during the opening of the sliding door. When the sliding door is fully closed, the origin $(x, y) = (0, 0)$ is defined as the coordinates (x_{A0}, y_{A0}) of the rotation fulcrum A. Then, the door's position can be expressed by the position of point A as $x = x_A$. To describe the coordinates (x_{B0}, y_{B0}) at the rotation fulcrum B, the angles θ and ϕ in Fig. A1 will be used in relation to the coordinates of the center point D at $(x, y) = (x_D, y_D)$ with the curvature radius R . The following equations can be used during the sliding door opening at $x = x_A$.

$$\theta = \tan^{-1} \frac{(y_B - y_{B0}) - a}{\sqrt{l^2 - ((y_B - y_{B0}) - a)^2}} \quad (\text{A6})$$

$$\phi = 90^\circ - (\theta + \varepsilon) \quad (\text{A7})$$

$$\varepsilon = \sin^{-1} \frac{y_D - (y_B - y_{B0})}{R - r} \quad (\text{A8})$$

As shown in Eqs. (A4) and (A5), the opening force $F_{Ax}(x_A)$ includes Eqs. (A6) to (A8). Note that the effect of the inertia force on the opening force $F_{Ax}(x_A)$ is small enough to be negligible.

Appendix B: Basic properties of wood materials and plywood

In Japanese Agricultural Standard (JAS), the strength and quality of wood-based structural materials are specified for each kind and grade, which are strictly examined and managed by the Registered Certification Organization. JAS collectively defines wood-based structural materials including structural lumber, structural laminated wood, structural laminated veneer lumber, structural plywood as structural materials (AIJ 2003, 2006). The materials whose qualities are constantly ensured by standards or manufacturing criteria are called structural materials. Additionally, the materials should have the structurally required strength, yield strength, stiffness, and toughness as

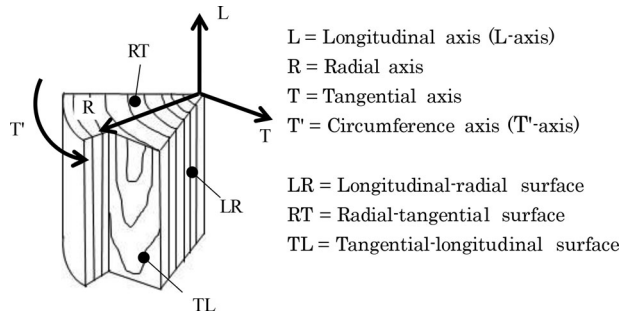


Figure B1. Axes and surfaces of wood.

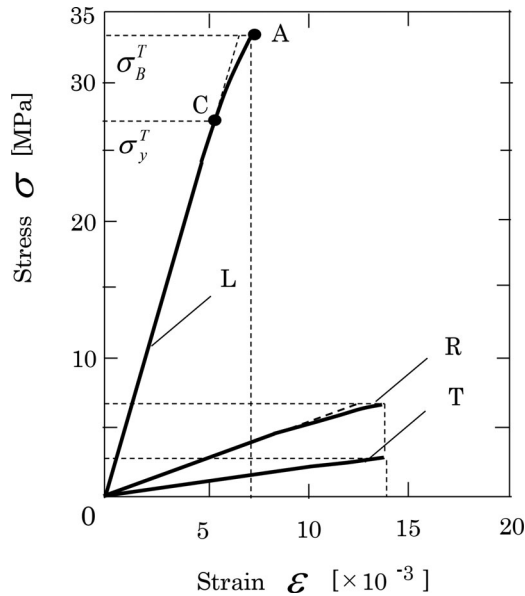


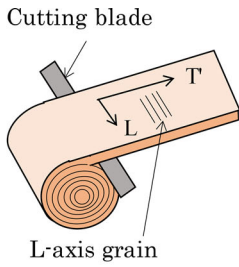
Figure B2. Tensile stress-strain diagram of sugi.

well as the durability to maintain the required capabilities through the service life (AIJ 2003, 2006). Among them, the structural lumber as well as the structural plywood related to the sliding door design are described below.

B1: Properties of structural lumber

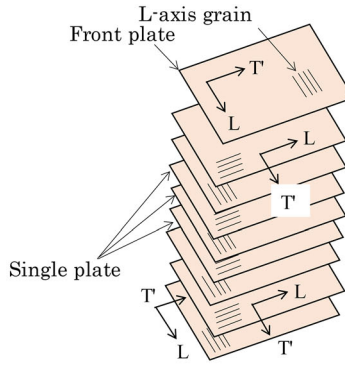
Structural lumber is the lumber that is made of softwood and aimed to be used for principal parts in structural designs. Lumber is approximately defined as the orthotropic materials that have three axes intersecting at right angles (Sawada 1959). Figure B1 illustrates the three axes and surfaces, and Fig. B2 shows the stress-strain diagram in a three-axis tensile test for sugi. Figure B2 summarizes the experimental data for the longitudinal axis (L), radial axis (R), and tangential axis (T) by Sawada (1959). In the figure, when the longitudinal axis (L) is taken as an example, the line segment OC is a straight range, and CA is a curved range. Point C and point A indicate the proportional limit and fracture point, respectively. The longitudinal axis (L) for sugi, softwood, shows a straight line until point C.

Comparing the stress-strain diagrams for the axes indicates that slopes corresponding to the modulus of elasticity are ordered in the longitudinal axis (L) > radial axis (R) > tangential axis (T), similar to the case of strength. JAS specifies the data for the longitudinal axis (L) but not for the radial axis (R) or tangential axis (T).



T'-axis : Circumference axis
 L-axis : Longitudinal axis

(a) Peeling a log into a single plate



(b) Nine-ply lamination of single plates

Figure B3. Creating and laminating single plate.

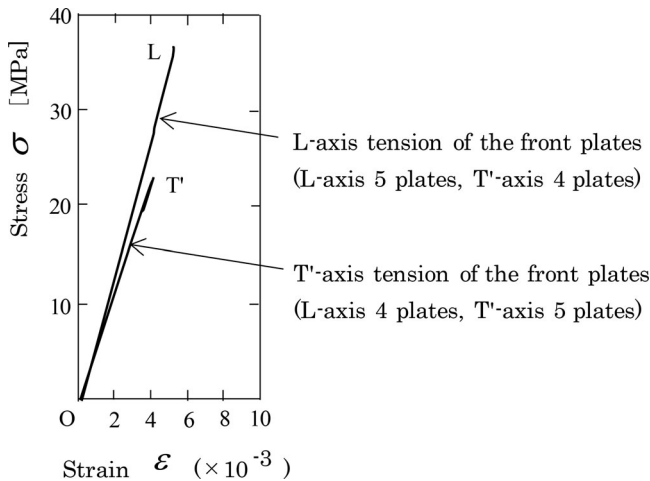
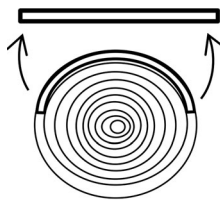
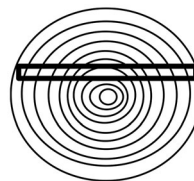


Figure B4. Tensile stress-strain diagram of lauan plywood (first-grade structural plywood).



(a) T'-axis



(b) T-axis

Figure B5. Explanatory drawing of T'- and T-axes.

B2: Properties of structural plywood

Plywood is a kind of composite board material where disadvantages of wood have been minimized, i.e., they are stronger than single-plate materials with wider board width and with less expansion and contraction. Additionally, the superior properties of wood are maintained including a humidity-control mechanism and workability. Structural plywood is designed to be used in areas where the strength can cause a problem. Since the strength of

Table B1. Comparing strength ratios of L-axis to T- or T'-axis using sugi, a lauan single plate, and lauan plywood.

Type of board	Static strength [MPa]			Strength ratio
	σ_B^L in L-axis	σ_B^T in T-axis	$\sigma_B^{T'}$ in T'-axis	
Sugi	33.3	2.63	–	$\sigma_B^T / \sigma_B^L = 0.08$
Lauan single plate	45.8	–	1.37	$\sigma_B^T / \sigma_B^L = 0.03$
Lauan plywood	36.4	–	23.6	$\sigma_B^T / \sigma_B^L = 0.65$

Table B2. Static tensile strength in L- and T'-axes by varying number of sugi plates N for first-grade C-C plywood in JAS (AIJ 2003, 2006).

Number of plates N	Plywood thickness t_p [mm]	Single plate thickness t_s [mm]	Static strength [MPa]			Strength ratio $\sigma_B^{T'} / \sigma_B^L$
			σ_B^L in L-axis (front plate)	$\sigma_B^{T'}$ in T'-axis (front plate)	$\sigma_B^{ave} = (\sigma_B^{T'} + \sigma_B^L) / 2$	
3	5.0	1.6	20.6	11.9	16.3	0.58
3	6.0	2.0	17.1	15.4	16.3	0.90
5	7.5	1.5	18.9	11.9	15.4	0.63
5	9.0	1.8	15.4	15.4	15.4	1.00
5	12.0	2.4	15.4	15.4	15.4	1.00
7*	15.0	2.1	11.9 (15.4) ^a	18.9 (15.4) ^a	15.4	1.59 (1.00) ^a
7	18.0	2.5	15.4	15.4	15.4	1.00
7	21.0	3.0	15.4	15.4	15.4	1.00
9	24.0	2.6	15.4	15.4	15.4	1.00
Average value			16.2	15.0	15.6	0.97

^aWhen the number of plates $N=7$ and plywood thickness $t_p = 15$ mm, the values (AIJ 2003, 2006) may have some misprints since $\sigma_B^{T'} / \sigma_B^L > 1$. Presumed correct values are indicated in parentheses.

structural plywood is directly linked to its manufacturing method, the following details the method. As shown in Fig. B3(a), a continuous thin plate is peeled from the log. Then, the resulting thin plates are laminated with glue as the grain direction of each plate is oriented perpendicular to that of adjacent plates and formed with pressure bonding (Fig. B3(b)). Figure B4 shows the tensile stress-strain diagram of structural plywood by Kuwamura (2010). The specimen is nine-ply (or plate) lauan plywood that is the first-grade structural plywood 21 mm thick (nominal) with the B-C grade surface quality. The test load directions are L-axis and T'-axis on the front plate, intersecting at right angles. The lines are almost straight, and their endpoints indicate the fracture points where brittle fracture occurs. Compared with the other lumbers, plywood has the characteristics such that the yield point does not clearly appear. In Figure B4, the tension in L-axis is higher than that in T'-axis because the number of plates is odd, and the plywood has one more L-axis plate, which gives higher strength than T'-axis plates. The number of plates is odd because the grain directions for the front and back plates need to be the same. Matching grain directions is used for appearance and shape stability. For the strength in different grain directions, JAS specifies the tensile strength values parallel and perpendicular to grain on the front plate. The following describes how much this laminate with odd plates affects the strength of plywood.

Table B1 compares the tensile strength of L-, T-, and T'-axes in sugi (Sawada 1959) and a lauan single plate (Kuwamura 2010) shown in Fig. B2. Table B1 also compares the tensile strength between L- and T'-axes for lauan plywood shown in Fig. B4. Figure B5(a) shows a cut out along with T'-axis, and Fig. B5(b) illustrates that along with T-axis. Table B1 indicates that both sugi and the lauan single plate show high anisotropy. The strength ratio of L to T in sugi is 0.08, and that of L to T' in the lauan single plate is 0.03. The tension in T- and T'-axes pulls against the grain of the growth rings, resulting in weaker strength. On the other hand, the lauan plywood in which L and T' are laminated alternately has the strength ratio (T'/L) of 0.65, indicating an approximate isotropic material. Therefore, plywood can mitigate anisotropy to improve the strength of raw wood.

Table B2 compares the static tensile strength in different grain directions on the front plate using the first-grade structural plywood C-C materials specified in JAS (AIJ 2003, 2006). Except for the thin plywood, the strength ratio $\sigma_B^{T'} / \sigma_B^L \cong 1$, and therefore the plywood can be considered to be isotropic. In Table B2, when the number of plate $N=7$ and plywood thickness $t_p = 15$ mm, the values (AIJ 2003, 2006) may have some misprints since σ_B^L in L-axis = 11.9 MPa < $\sigma_B^{T'}$ in T'-axis = 18.9 MPa. The presumed correct results $\sigma_B^L = 18.9$ MPa > $\sigma_B^{T'} = 11.9$ MPa are shown in parentheses. Note that usually $\sigma_B^L = 15.4$ MPa for $N=5$ to 9 except for $N=7$ and $t_p = 15$ mm.

The value $\sigma_B^L = 11.9$ MPa in Table B2 was used as the tensile strength of plywood in Table 2 in Section 4.1. This tensile strength $\sigma_B^T = 11.9$ MPa in Table 2 was used in Fig. 14 to obtain the yield stress as $\sigma_y^T = \sigma_B \times \alpha_{a2} = 7.8$ MPa and the fatigue limit as $\sigma_w = \sigma_B \times \alpha_f = 2.5$ MPa. If σ_B^L in L-axis = 11.9 MPa is a misprint, the correct

Table C1. Method for calculating σ_w/σ_B from coefficients α_a to α_f defined in ASTM and AIJ when load duration is 50 years^d.

Coefficients	Bending		Tension parallel to grain		Compression parallel to grain	
	ASTM	AIJ	ASTM	AIJ	ASTM	AIJ
(a) Adjustment factor α_a in ASTM, $\alpha_a = (a1) \times (a2)$ in AIJ (Factor affected by changing the load duration to 50 years)	1/2.1	1/2.7	1/2.1	1/2.7	1/1.9	1/2.7
(a1) Degradation factor α_{a1} in ASTM and AIJ (Factor affected by changing the load duration to 50 years)	0.6	0.55	0.6	0.55	0.6	0.55
(a2) Safety factor α_{a2} in AIJ (equivalent to $\sigma_y/\sigma_B =$ ratio of yield strength to static strength ($\alpha_{a2} = \sigma_y/\sigma_B$))	(1/1.25) ^a	2/3	(1/1.25) ^a	2/3	(1/1.14) ^a	2/3
(b) Strength ratio α_b prescribed in ASTM	1.0	(1.0) ^a	1.0 \times 0.55	(1.0) ^a	1.0	(1.0) ^a
(c) Seasoning adjustment α_c prescribed in ASTM	1.0	(1.0)	1.0	(1.0)	1.0	(1.0)
(d) Environmental coefficient α_d prescribed in AIJ	(3/4) ^b	3/4	(6/7) ^b	6/7	(6/7) ^b	6/7
(e) Special factors α_e prescribed in ASTM	1.0	(1.0) ^a	(1.0) ^a	(1.0) ^a	(1.0) ^a	(1.0) ^a
(f) Product of coefficients $\alpha_f = \alpha_a \times \alpha_b \times \alpha_c \times \alpha_d \times \alpha_e$ (Equivalent to $\sigma_w/\sigma_B =$ ratio of alternating fatigue limit to static strength ($\sigma_w/\sigma_B = \alpha_f$)) (Factor affected by changing the load duration to 50 years)	0.36	0.27^c	0.22^c	0.31	0.45	0.31^c
(g) Product of coefficients α_f for the load duration of 250 years	0.34	0.25^c	0.21^c	0.29	0.43	0.29^c

Values are for plywood made of soft wood

^aValues not prescribed in ASTM or AIJ are in parentheses.

^bSince α_d value for plywood is not prescribed in ASTM, the value in AIJ is indicated.

^cThe values recommended by the authors are shown in **bold** type.

^dAlthough the values in this table are for the first-grade structural plywood material 15 mm thick made of softwood (sugi) specified in JAS, this method can be applied to plywood made of hardwood.

tensile stress can be $\sigma_B^T = 15.4$ MPa, which is 1.3 times larger than $\sigma_B^T = 11.9$ MPa, and the yield stress σ_y^T and the fatigue limit σ_w are also estimated 1.3 times larger. Then, the fatigue risk evaluated from Fig. 14 is reduced, and the smallest safety factor SF = 4.4 in Table 4 becomes about 1.3 times larger (see Fig. 14).

Appendix C:

Product of coefficients α_f equivalent to ratio of fatigue limit to static strength σ_w/σ_B when load duration is 50 years

Compared with the load duration of 250 years required for load-bearing structures of buildings, the load duration of 50 years is considered to be enough for doors because they are mechanical structures that can be easily replaced. To verify the difference, the products of coefficients α_f for the load durations of 250 years and 50 years are shown in Table C1 to be compared.

First, the values of degradation factor α_{a1} are read from Fig. 5: $\alpha_{a1} = 0.6$ in ASTM; $\alpha_{a1} = 0.55$ in AIJ. Then the values of adjustment factor α_a are obtained setting the values for safety factor α_{a2} to the same as those for the load duration of 250 years. The values of product of coefficients α_f for the load duration of 50 years are obtained: $\alpha_f = 0.22$ to 0.45. Compared to those for 250 years, $\alpha_f = 0.21$ to 0.43, the load duration of 250 years has a 5% to 6% advantage, indicating that the difference is small.